Pis'ma v ZhETF, vol. 83, iss. 10, pp. 519 – 524

Formation and Dynamics of Relativistic Electromagnetic Solitons in Plasmas Containing High and Low-Energy Electron Components

B. Eliasson, P. K. Shukla

Institut für Theoretische Physik IV, Fakultät für Physik und Astronomie, Ruhr-Universität Bochum, D-44780 Bochum, Germany

Submitted 22 March 2006
Resubmitted 10 April 2006

We present theoretical and numerical studies of the nonlinear interactions between intense electromagnetic waves in plasmas containing high and low-energy electron components. Such plasmas are frequently observed in laser-plasma experiments, where the hot electron component is created by the acceleration of electrons by strong electrostatic waves that are created by the laser induced Raman forward and backward instabilities. The two-component electron plasma is described by the Vlasov equation for the hot electrons and the hydrodynamic equations for the cold electrons, which are coupled nonlinearly with the electromagnetic wave equation and the Poisson equation for the potential. The present nonlinear system is shown to admit electromagnetic solitary waves correlated with a positive potential and trapped electron islands from the hot electron population.

PACS: 52.35.–g, 52.38.Dx

In a non-equilibrium plasma, the nonlinear saturation mechanism for large amplitude plasma waves is usually the particle trapping and collisionless heating of the electrons involving wave-particle interactions. Laser-plasma experiments [1 – 3] as well as theoretical and numerical studies [4 – 7] have demonstrated the formation of non-thermal electron distributions via stimulated Raman scattering of electromagnetic waves off nonlinear kinetic electron acoustic wave-modes involving trapped electrons/electron holes. In the long wavelength limit, the presence of intense electromagnetic waves in plasmas may lead to a three-dimensional collapse of both electromagnetic and Langmuir waves [8]. The relativistic mass increase in the electromagnetic fields also play an important role for numerous parametric instabilities (e.g. the modulational and Raman forward and backward scattering instabilities [9 – 13]), and for the localization of electromagnetic waves in the form of envelope solitons [14 – 16] within the framework of the Maxwell and hydrodynamic equations. Kinetic effects associated with trapping of electrons in the electrostatic field in hot plasmas give rise to relativistic electron holes (REHs) [17], which significantly affect the localization of intense electromagnetic waves (EMWs) [18]. Both in laboratory [19] and space plasmas [20], one frequently encounters electron distributions that can be described as a superposition of two distinct temperatures [21]. The nonlinear interactions between intense EMWs and two-component electron plasmas can give rise to new classes of parametric instabilities [22] and coherent electromagnetic wave structures [23]. The trapping of electrons in the self-consistent electrostatic potential is the basic mechanism for the electron holes [24, 25]. Non-relativistic electron holes have been excited in laboratory experiments by different techniques [26 – 28].

In this Letter, we consider for the first time the nonlinear interactions between intense electromagnetic waves and plasma containing two distinct groups of electrons. The two electron populations are composed of a low-energy component which is described by the relativistic electron hydrodynamic equations, while the high-energy hot electron component is modelled by the relativistic Vlasov equation. The EMWs are coupled with the plasma slow motions, supported by the cold and hot electron components, via the relativistic ponderomotive force and the Poisson equation. We seek stationary solutions of the governing nonlinear system of equations in order to understand the interplay between the cold and hot electron components on the formation of intense electromagnetic envelope solitons. The stability of the coupled REH-EMW envelope soliton has also been investigated, by means of direct simulations of the Vlasov–Maxwell system of equations.

We first present the relevant nonlinear equations describing the action of intense EMWs on the hot and cold electron components in a collisionless plasma. We shall deal with the electromagnetic wave localization on a short timescale, so that the ions do not have time to respond to electromagnetic and electrostatic fields in our plasma. At equilibrium, we have $n_{i0} = n_{eh0} + n_{ec0} \equiv \equiv n_{e0}$, where n_{j0} is the unperturbed particle density of the species j (j equals i for the ions, e for the electrons, and eh and ec for the hot and cold electrons, respectively). The EMWs cause relativistic electron mass increase, and produce electron density perturbations on account of the radiation relativistic ponderomotive force $F = -m_e c^2 \partial\gamma/\partial z$, where m_e is the electron rest mass, c is the light speed and $\gamma = (1 + p_z^2/m_e^2c^2 + e^2|\mathbf{A}|^2/m_e^2c^4)^{1/2}$ is the relativistic gamma factor. Here, p_z is the z component of the electron momentum, $\mathbf{A}$ is the perpendicular (to $\hat{\mathbf{z}}$, where $\hat{\mathbf{z}}$ is the unit-vector along the z direction in a Cartesian coordinate system) component of the vector potential of the circularly polarized EMWs, and e is the magnitude of the electron charge. The dynamics is governed by the wave equation for the EMW, the relativistic Vlasov equation for the hot electrons, and the continuity and relativistic momentum equations for the cold electrons, respectively,

$$\frac{\partial^2 \mathbf{A}}{\partial t^2} - \frac{\partial^2 \mathbf{A}}{\partial z^2} + \Omega^2 \mathbf{A} = 0, \tag{1}$$

$$\frac{\partial f_h}{\partial t} + \frac{p_z}{\gamma_h}\frac{\partial f_h}{\partial z} + \frac{\partial(\phi - \gamma_h)}{\partial z}\frac{\partial f_h}{\partial p_z} = 0, \tag{2}$$

$$\frac{\partial N_c}{\partial t} + \frac{\partial}{\partial z}(N_c V_{cz}) = 0, \quad V_{cz} = \frac{P_{cz}}{\gamma_c}, \tag{3}$$

$$\frac{\partial P_{cz}}{\partial t} + \frac{\partial \gamma_c}{\partial z} = \frac{\partial \phi}{\partial z}, \tag{4}$$

together with the Poisson equation for the electrostatic potential

$$\frac{\partial^2 \phi}{\partial z^2} = \mu \int_{-\infty}^{\infty} f_h \, dp_z + (1-\mu) N_c - 1, \tag{5}$$

where $\Omega^2 = \mu \int_{-\infty}^{\infty} (f_h/\gamma_h)\, dp_z + (1-\mu) N_c/\gamma_c$ represents the square of the local electron plasma frequency that accounts for the electron density variation and the relativistic electron mass increase, $\mu = n_{eh0}/n_{e0}$, and $\alpha = V_{Teh}/c$ where $V_{Teh} = (T_{eh}/m_e)^{1/2}$ is the electron thermal speed, and T_{eh} is the temperature of the hot electrons. The vector potential $\mathbf{A}$ is normalized by $m_e c/e$, the scalar potential ϕ by $m_e c^2/e$, the momenta p_z and P_{cz} by $m_e c$, the hot electron distribution function f_h by n_{h0}/c, the cold electron density N_c by n_{ec0}, the space z by c/ω_{pe}, and the time t by ω_{pe}^{-1}, where $\omega_{pe} = (4\pi n_{i0} e^2/m_e)^{1/2}$ is the electron plasma frequency. The gamma-factors for the hot and cold electrons are $\gamma_h = (1 + p_z^2 + |\mathbf{A}|^2)^{1/2}$ and $\gamma_c = (1 + P_{cz}^2 + |\mathbf{A}|^2)^{1/2}$, respectively. In Eq. (1), we have used the Coulomb gauge $\nabla \cdot \mathbf{A} = 0$, and have excluded the longitudinal (z-) component $\partial^2\phi/\partial t \partial z = j_z$, where j_z is the parallel electron current density, by noticing that this component is equivalent to the Poisson equation (5) [18].

We now investigate the properties of driven REHs, which move with the constant speed v_0 relative to the observer (bulk plasma) frame. We assume that N_c, P_{cz} and ϕ depend on $\xi = z - v_0 t$ only, where v_0 is the constant propagation speed, and that f_h depends on (ξ, p_z) so that Ω is a function of ξ only. By using the ansatz $\mathbf{A} = (1/2)W(\xi)(\hat{\mathbf{x}} + i\hat{\mathbf{y}})\exp[-i(\omega_0 + \theta)t + i(k_0 + K)z] +$ +complex conjugate, where W is a real-valued function, we then obtain $K = \omega_0(v_0 - v_g) + v_0\theta$, and Eq. (1) can be written as

$$\frac{d^2 W}{d\xi^2} - \lambda W - \gamma_0^2 \left(\Omega^2 - \Omega_p^2\right) W = 0, \tag{6}$$

where $\omega_0 = (\Omega_p^2 + k_0^2)^{1/2}$ is the EMW frequency, $\Omega_p^2 = \mu \int_{-\infty}^{\infty} \widetilde{f}_0(p_z)/\sqrt{1+p_z^2}\, dp_z + 1 - \mu =$ $= \mu K_0(\alpha^{-2})/K_1(\alpha^{-2}) + 1 - \mu$ is the normalized (by ω_{pe}) relativistic plasma frequency at equilibrium, K_0 is a modified Bessel function of second kind, $v_g = k_0/\omega_0$ is the group speed. Here $\lambda = -\theta^2 - 2\omega_0\theta + \gamma_0^2\omega_0^2(v_0^2 - v_g^2)$ represents a nonlinear eigenvalue of Eq. (6), where we have denoted $\gamma_0 = 1/\sqrt{1 - v_0^2}$. Below, we will restrict ourselves to the case $v_g = v_0$ so that $k_0 = \gamma_0 v_0 \Omega_p$, $\omega_0 = \gamma_0 \Omega_p$ and we have $K = v_0\theta$ and the nonlinear frequency shift $\theta = -\omega_0 + (\omega_0^2 - \lambda)^{1/2}$. The gamma factors are now expressed as $\gamma_h = (1 + p_z^2 + W^2)^{1/2}$ and $\gamma_c = (1 + P_{cz}^2 + W^2)^{1/2}$. Equations (3) and (4) can be integrated to obtain $-v_0 N_c + N_c V_{cz} = -v_0$ and $-v_0 P_{cz} + \gamma_c - 1 - \phi = 0$, respectively, where we have used the boundary conditions $N_c = 1$, $P_{cz} = 0$, $|\mathbf{A}| = 0$ and $\phi = 0$ at $|\xi| = \infty$. We thus have the density $N_c = v_0/(v_0 - V_{cz})$, where $V_{cz} = P_{cz}/(1 + P_{cz}^2 + W^2)^{1/2}$ and the momentum $P_{cz} = \gamma_0^2 v_0(1+\phi) - \sigma\gamma_0[\gamma_0^2(1+\phi)^2 - 1 - W^2]^{1/2}$, where $\sigma = 1$ ($\sigma = -1$) for $v_0 > 0$ ($v_0 < 0$). Equation (2) takes the form

$$\left(-v_0 + \frac{p_z}{\gamma_h}\right)\frac{\partial f_h}{\partial \xi} + \frac{d(\phi - \gamma_h)}{d\xi}\frac{\partial f_h}{\partial p_z} = 0, \tag{7}$$

and the Poisson Eq. (5) becomes

$$\frac{d^2\phi}{d\xi^2} = \mu \int_{-\infty}^{\infty} f_h \, dp_z + (1-\mu) N_c - 1. \tag{8}$$

Using the technique outlined in Ref. [18], an exact solution of Eq. 7 can be constructed of the form

$$f_h = \begin{cases} a_0 \exp\left[-\alpha^{-2}\left(\sqrt{1+\widetilde{p}_+^2(\mathcal{E}_h)} - 1\right)\right], & p > p_+, \\ a_0 \exp\left[-\alpha^{-2}(\gamma_0 - 1 + \beta\mathcal{E}_h)\right], & p_- \le p \le p_+, \\ a_0 \exp\left[-\alpha^{-2}\left(\sqrt{1+\widetilde{p}_-^2(\mathcal{E}_h)} - 1\right)\right], & p < p_-, \end{cases} \tag{9}$$

where $\mathcal{E}_h = -v_0 p_z + \gamma_h - 1/\gamma_0 - \phi$ is the conserved energy of the electron trajectories of Eq. (7). The separatrices

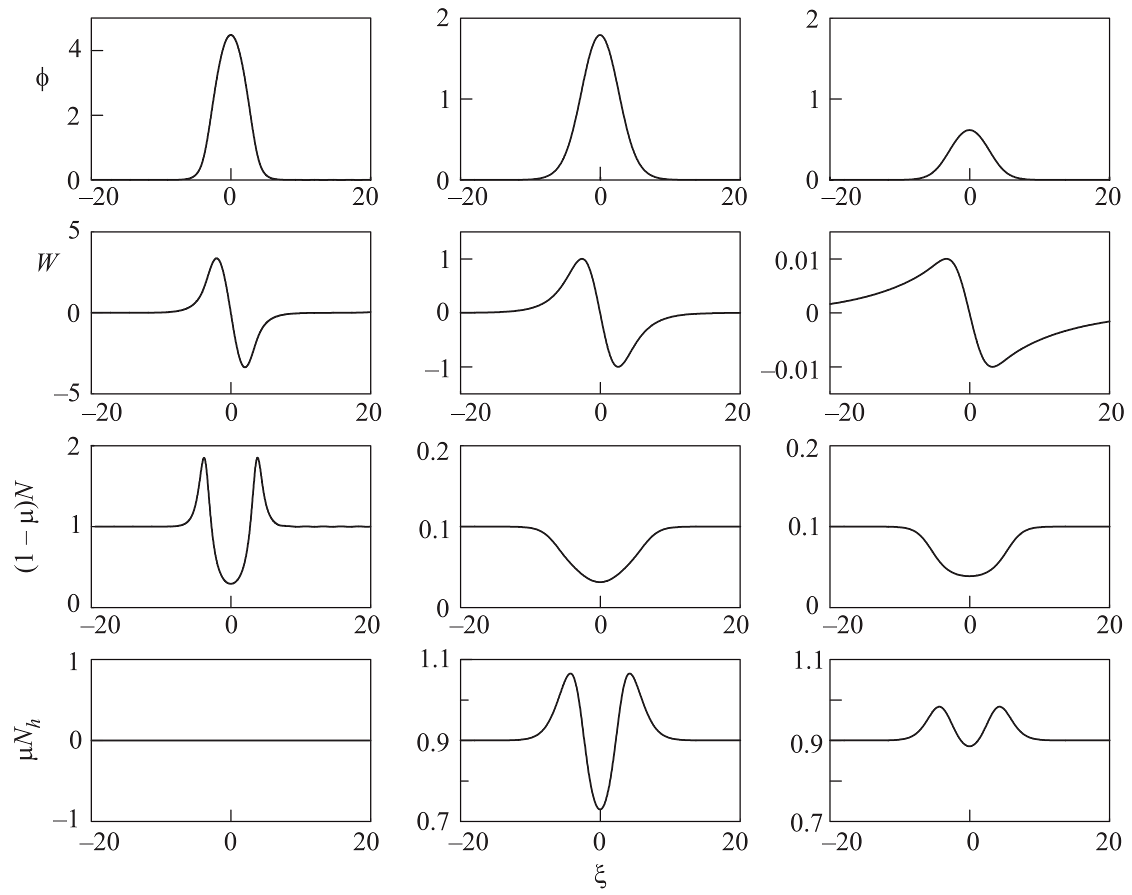

Fig.1. The profile of the potential, the EMW envelope, and the cold and hot electron number densities (upper to lower panels) associated with a cold plasma EMW soliton (left panels) and a REH-EMW soliton with large-amplitude trapped EMWs (middle panels) and a REH-EMW soliton with small-amplitude trapped EMWs (right panels), propagating with the speed $v_0 = 0.4$. The total electron density is $N_e = \mu N_{eh} + (1-\mu)N_{ec}$. Parameters for the EMW soliton (left panels) are: $\mu = 0$, and $\lambda = 0.4592$. The REH-EMW soliton (middle panels): $\mu = 0.9$, $\alpha = 0.4$, $W_{\max} = 1.0$, and $\lambda = 0.224$. The bare REH (right panels): $\mu = 0.9$, $\alpha = 0.4$, $W_{\max} = 0.01$, and $\lambda = 0.0114$

in momentum space between the free and trapped electrons, $p_{\pm} = \gamma_0 v_0 (\gamma_0\phi + 1) \pm \gamma_0[(\gamma_0\phi + 1)^2 - 1 - W^2]^{1/2}$, are obtained by setting $\mathcal{E}_h = 0$ and solving for p. The distribution function for the trapped electrons (in the interval $p_- < p < p_+$) is characterized by the trapping parameter β, which gives an excavated distribution function for negative values. We note that when $\phi = W = 0$ far away from the REH, then $p_+ = p_-$ and the number density of the trapped electrons vanishes. The functions $\widetilde{p}_{\pm}(\mathcal{E}_h) = \gamma_0 v_0 (\gamma_0\mathcal{E}_h + 1) \pm \gamma_0[(\gamma_0\mathcal{E}_h + 1)^2 - 1]^{1/2}$ are chosen so that they take the value p where $\phi = W = 0$, and thus the electron distribution function (9) equals the Jüttner-Synge distribution function [29] $\widetilde{f}_0(p_z) = a_0 \exp[-(\sqrt{1+p_z^2} - 1)/\alpha^2]$, far away from the REH, where the normalization constant is $a_0 = \{\int_{-\infty}^{\infty} \exp[-(\sqrt{1+p_z^2} - 1)/\alpha^2]\, dp_z\}^{-1} = \exp(-\alpha^{-2})/2K_1(\alpha^{-2})$, where K_1 is a modified Bessel function of second kind. Integrating the distribution function (9) over the momentum space, we obtain the total electron number density as a function of ϕ and W, which are calculated self-consistently by means of the Poisson and Schrödinger equations, respectively.

We have solved the coupled Schrödinger and Poisson system of Eqs. (6) and (8) numerically, and have displayed in Fig.1 the resulting profiles of the potential ϕ, the EMW envelope W and the hot and cold electron number densities, both for the case with only cold electrons and for the case with 90% hot electrons and 10% cold electrons ($\mu = 0.9$). Both EMW solitons in a cold plasma [16] and trapped EMW envelopes in a REHs [18] can have different levels of excited states where the ground state has a symmetric, bell-shaped envelope, the first excited state has an anti-symmetric envelope with one maximum and one minimum, etc. Here, we consider a scenario in which the EMW envelope has an anti-symmetric maximum and minimum, and will discuss the similarities and differences between the cold plasma soliton and the REH-EMW soliton. Both the cold plasma soliton and REH-EMW soliton are associated with a large-amplitude positive potential, which can trap the electrons. In the case of only cold electrons, all electrons are free and we do not have any trapped electrons, but when a hot electron population is included, some of the thermal electrons will be trapped in the potential hump. The question remains whether these two types of solitary waves are fundamentally different or whether they are the same kind of localized EMWs, but in different parameter regimes. One difference between the two cases is that the electromagnetic envelope soliton involving only cold electrons has a point spectrum, i.e. for a given speed of the EMW soliton there is one eigenvalue λ and one amplitude/shape of the EMW envelope (see the left panels in Fig.1), while for the REH-EMW soliton there is a continuous range of values on λ depending on the amplitude of the EMW envelope (see the middle and right panels of Fig.1). Another difference is that the electron trajectories have a different topology for the two cases, which is illustrated by following the trajectory for a test electron in phase space. The relativistic equation of motion for the test electron has the conserved energy integral $-v_0 p_z + \gamma - 1 - \phi = \mathcal{E}$, which for $\mathcal{E} = 0$ gives the electron momentum that equals the cold fluid momentum, $p_z = P_{cz}$, and for $\mathcal{E} = 1/\gamma_0 - 1$ gives the separatrix $p = p_\pm$ between trapped and free electrons in the REH solution discussed above. In Fig.2a, we have assigned different values of $\mathcal{E}$ for an EMW soliton in a cold plasma. The dotted curve illustrates a test electron with the same energy ($\mathcal{E} = 0$) as for the cold fluid particles, yielding $p_z = P_{cz}$. The solid line represents the separatrix between the trapped and free electrons in a REH for which $\mathcal{E} = 1/\gamma_0 - 1 \approx -0.0835$. Finally, The dashed lines is for $\mathcal{E} \approx -0.0455$, which is the largest energy that trapped or reflected electrons can have; larger energies are responsible for free (untrapped and unreflected) electrons, and lower energies are associated with either trapped electrons inside the solitary pulse or reflected electrons on either side of the electromagnetic pulse. In Fig.2b, we have used the fields obtained for an REH-EMW soliton and calculated the particle trajectories for a test electron. Here, the solid curve, for $\mathcal{E} = 1/\gamma_0 - 1 \approx -0.0835$, describes the separatrix between trapped and free electrons in the REH-EMW soliton. We see that the width of the trapped region vanishes for large values of $|\xi|$, and we do not have any reflected electrons. We thus note that the localized structures are fundamentally different for the cold plasma soliton and the REH-EMW soliton cases. The cold plasma EM soliton will reflect thermal electrons

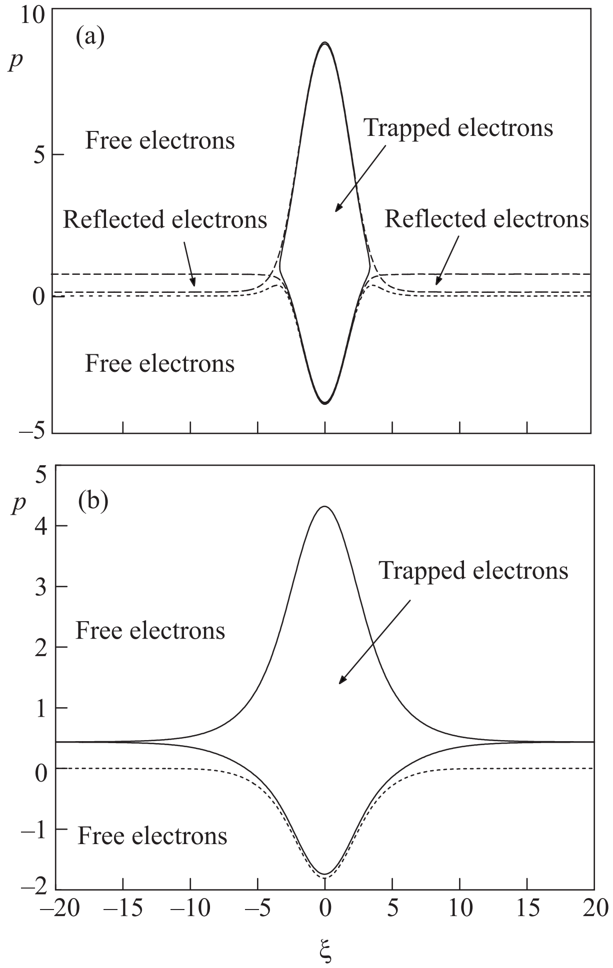

Fig.2. (a) Separatrices between trapped, reflected and free particles for a cold plasma EMW soliton, indicated with dashed lines. The solid line shows the value of the functions $p_\pm(\phi, W)$. Parameters are: $v_0 = 0.4$, $\mu = 0$, $\lambda = 0.4592$. The dotted line indicates the cold fluid momentum $P_{cz}(W, \phi)$. (b) Separatrix between trapped and free electrons for a REH-EMW soliton, given by the function $p_\pm(\phi, W)$. Parameters are: $v_0 = 0.4$, $\mu = 0.9$, $\alpha = 0.4$, and $\beta = -0.5$. The EMW amplitude was $W_{\max} = 1.0$, giving $\lambda = 0.224$. The dotted line indicates the cold fluid momentum $P_{cz}(W, \phi)$

that are traveling with a speed close to the soliton speed, and the soliton will lose energy to those electrons. Thus, the cold plasma EMW soliton has a long-range effect in the plasma via the reflected regions indicated in Fig.2a. As a contrast, the REH-EMW soliton has no reflected electrons, but only a population of trapped electrons which are absent far away from the soliton. This soliton is thus more "localized", and turns out to be more stable than the cold plasma EMW soliton.

We have investigated how the inclusion of a cold plasma population influences the REH-EMW soliton, by

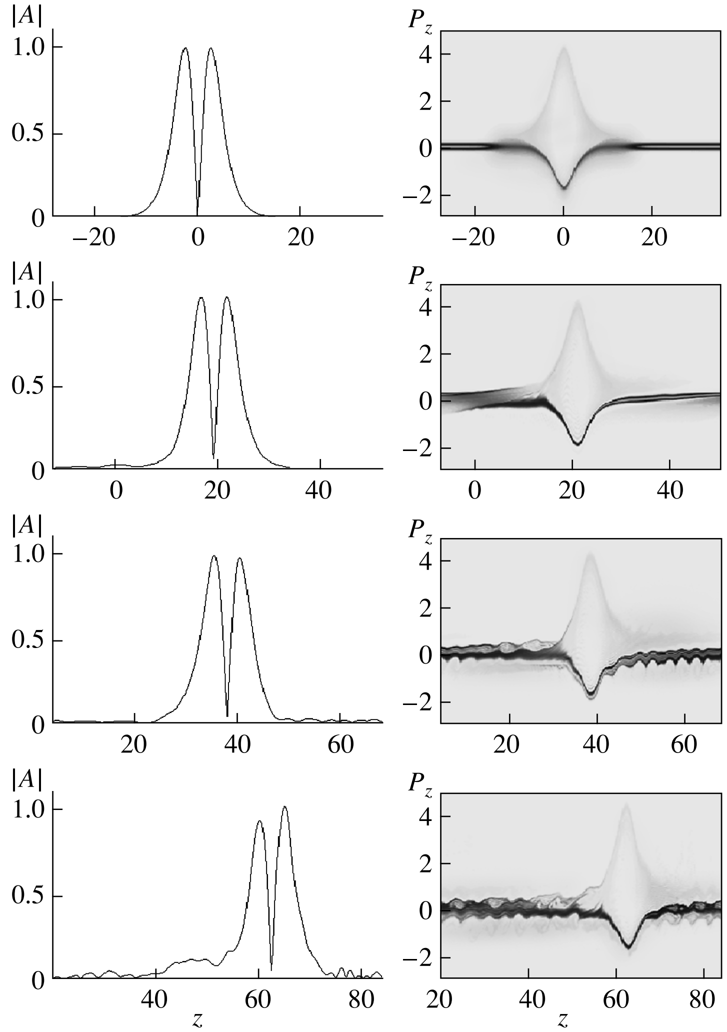

Fig.3. The modulus of the electromagnetic field $|A|$ (left panels) and phase plots of the electron distribution function f (right panels) at times $t = 0$, $t = 50$, $t = 100$, and $t = 150$ (upper to lower panels). At time $t = 0$, the plasma surrounding the REH-EMW soliton has the parameters $v_0 = 0.4$, $\mu = 0.9$, $\alpha = 0.4$, and $\beta = -0.5$, $W_{\max} = 1.0$ (cf. Fig.2), while the plasma at $|z| > 20$ is colder with $\alpha = 0.1$

solving the coupled system of Eqs. (6) and (8) for different values of $\mu = n_{eh0}/n_{e0}$. Below a critical value of $\mu \approx 0.8$, we could not find numerical solutions for localized REH-EMW solitons of the type shown in Fig.2b. In order to investigate the robustness of a REH-EMW soliton, we have numerically solved, by using the methods developed in Ref. [18], the time-dependent Vlasov-Maxwell-Poisson system of Eqs. (1), (2) and (5)for a REH-EMW soliton that travels from a region containing a small fraction of cold electrons, $\mu = 0.9$, into a region having only cold electrons, $\mu = 0$. The cold electrons have $\alpha = 0.1$ and the hot electrons have $\alpha = 0.4$. The numerical result is displayed in Fig.3, where we see that the EH is quite robust against streams of cold electrons and wave turbulence, and so is the EMW envelope. However, small-amplitude EMWs are leaving the REH in its trailing end at the latest time when the REH has entered the cold plasma region. In simulations with only hot electrons, the REH-EMW soliton is very robust and does not show any signature of instability. The robustness of the REH-EMW solitons is in line with experiments with non-relativistic electron holes [26, 28] that are very long-lived, despite the three-dimensional geometry of the experiments.

In conclusion, we have presented new results dealing with the localization and dynamics of intense electromagnetic waves that nonlinearly interact with plasmas containing two distinct groups of electrons. The latter are common in laser produced plasmas as well as in space where electron distribution functions are often non-Maxwellian. Our numerical results reveal new features of electromagnetic envelope solitons due to an interplay between the hot and low electron components. Our computer simulations of the Maxwell-Vlasov-Poisson system demonstrate the robustness of the intense localized electromagnetic pulses accompanied with localized electrostatic potentials associated with enhanced charge separation that is created by relativistic ponderomotive force of localized light.

This work was partially supported by the Deutsche Forschungsgemeinschaft through the Sonderforschungsbereich 591 entitled "Universelles Verhalten Gleichgewichtsferner Plasmen: Heizung, Transport und Strukturbildung".

1. D. S. Montgomery, R. J. Focia, H. A. Rose et al., Phys. Rev. Lett. **87**, 155001 (2001).
2. D. S. Montgomery, J. A. Cobble, J. C. Fernández et al., Phys. Plasmas **9**, 2311 (2002).
3. J. L. Kline, D. S. Montgomery, B. Bezzerides et al., Phys. Rev. Lett. **94**, 175003 (2005).
4. H. A. Rose and D. A. Russell, Phys. Plasmas **8**, 4784 (2001).
5. Lj. Nikolić, , M. M. Škorić, S. Ishiguro, and T. Sato, Phys. Rev. E **66**, 036404 (2002).
6. H. X. Vu, L. Yin, D. F. DuBois et al., Phys. Rev. Lett. **95**, 245003 (2005).
7. L. Yin, W. Daughton, B. J. Albright et al., Phys. Rev. E **73**, 025401(R) (2006).
8. E. A. Kuznetsov, Sov. Phys. JETP **39**, 1003 (1974). [Zh. Eksp. Teor. Fiz. **66**, 2037 (1974).]
9. L. Stenflo, Phys. Scr. **14**, 320 (1976); ibid. **23**, 779 (1981); L. O. Silva et al., Phys. Rev. Lett. **83**, 2703 (1999).
10. C. J. McKinstrie and R. Bingham, Phys. Fluids B **4**, 2626 (1992).
11. A. S. Sakharov and V. I. Kirsanov, Phys. Rev. E **49**, 3274 (1994).
12. S. Guerin, G. Laval, P. Mora et al., Phys. Plasmas **2**, 2807 (1995).
13. C. D. Decker, W. B. Mori, K.-C. Tzeng, and T. Katsouleas, Phys. Plasmas **3**, 2047 (1996).
14. P. K. Shukla, M. Y. Yu, and N. L. Tsintsadze, Phys. Fluids **27**, 327 (1984); P. K. Shukla and L. Stenflo, Phys. Rev. A **30**, 2210 (1984).
15. P. K. Shukla, N. N. Rao, M. Y. Yu, and N. L. Tsintsadze, Phys. Rep. **138**, 1 (1986); R. Bingham, J. T. Mendonça, and P. K. Shukla, Plasma Phys. Control. Fusion **46**, R1 (2004).
16. P. K. Kaw, A. Sen, and T. Katsouleas, Phys. Rev. Lett. **68**, 3172 (1992); V. Saxena, A. Das, A. Sen, and P. Kaw, Phys. Plasmas **13**, 032309 (2006).
17. B. Eliasson and P. K. Shukla, Phys. Lett. A **340**, 237 (2005); Phys. Rep. **422**, 225 (2006).
18. P. K. Shukla and B. Eliasson, Phys. Rev. Lett. **94**, 065002 (2005).
19. W. D. Jones, A. Lee, S. M. Gleman, and H. J. Doucet, Phys. Rev. Lett. **35**, 1349 (1975).
20. R. E. Ergun, Y.-J. Su, L. Andersson et al., Phys. Rev. Lett. **87**, 045003 (2001).
21. M. Y. Yu and P. K. Shukla, J. Plasma Phys. **29**, 409 (1983).
22. P. K. Shukla and M. A. Hellberg, J. Plasma Phys. **67**, 363 (2002).
23. P. K. Shukla, L. Stenflo, and M. Hellberg, Phys. Rev. E **66**, 027403 (2002).
24. S. Bujarbarua and H. Schamel, J. Plasma Phys. **25**, 515 (1981).
25. H. Schamel, Phys. Rep. **140**, 161 (1986).
26. K. Saeki, P. Michelsen, H. L. Pécseli, and J. J. Rasmussen, Phys. Rev. Lett. **42**, 501 (1979).
27. G. Petraconi and H. S. Maciel, J. Phys. D **36**, 2798 (2003).
28. W. Bertsche, J. Fajans, and L. Friedland, Phys. Rev. Lett. **91**, 265003 (2003).
29. S. R. de Groot, *Relativistic Kinetic Theory, Principles and Applications*, North-Holland, Amsterdam, 1980.